American Mineralogist, Volume 77, pages 244–250, 1992

A new interatomic potential model for calcite: Applications to lattice dynamics studies, phase transition, and isotope fractionation

MARTIN T. DOVE, BJÖRN WINKLER*
Department of Earth Sciences, University of Cambridge, Downing Street, Cambridge CB2 3EQ, U.K.
MAURICE LESLIE
Daresbury Laboratory, Warrington, Cheshire WA4 4AD, U.K.
MARK J. HARRIS, EKHARD K. H. SALJE
Department of Earth Sciences, University of Cambridge, Downing Street, Cambridge CB2 3EQ, U.K.

ABSTRACT

A microscopic model for calcite and aragonite has been developed that includes short range repulsive atom-atom interactions; two-, three-, and four-body potentials; and long-range Coulomb interactions. The structures and elastic constants of both phases are reproduced satisfactorily, as are the phonon frequencies for calcite. The observed softening of a transverse acoustic phonon in the [1,0,4] direction in calcite is reproduced by our model. Applications of the model include the calculation of reduced fractionation coefficients for $^{16}O/^{18}O$ of calcite and isotope exchange coefficients of calcite and H_2O that are in reasonably good agreement with experimental data. The lattice parameters of the high-temperature disordered phase of calcite have been calculated and are in good agreement with experimental data. It is inferred that the temperature dependence of the spontaneous strain accompanying the phase transition in calcite is due to short range order of the CO_3 groups, which also explains the anomalous negative thermal expansion along [100].

INTRODUCTION

The mineral calcite ($CaCO_3$, space group $R\bar{3}c$, $Z = 2$) is important in many areas across the whole field of the Earth sciences. Examples are the orientational order-disorder phase transition at 1260 K (Dove and Powell, 1989) and the use of the isotope fractionation ($^{12}C/^{13}C$ and $^{16}O/^{18}O$) of calcite in geochemistry. The aim of the present study is to develop a microscopic interatomic potential model for $CaCO_3$ that can be used to give thermodynamic information for such applications.

A number of models for calcite have already appeared in the literature. The majority of these are harmonic force-constant models aimed at reproducing the observed phonon dispersion curves (e.g., Cowley and Pant, 1973). However, force-constant models are always so specific to the particular crystal structure that their only application is for the calculation of the phonon densities of states, and they cannot be applied to any other polymorphs of $CaCO_3$. More recently Singh et al. (1987) proposed an interatomic potential model for calcite. Unfortunately, on close inspection it appears that this model does not give reasonable calculated phonon frequencies. Moreover, this model does not allow any flexibility of the carbonate molecular ion, which we consider to be important for certain applications. We have therefore chosen to develop a new model for $CaCO_3$ with the aim of obtaining reasonable agreement with a wide variety of observed properties.

We have a number of applications for our new model. One immediate application is for the interpretation of recent inelastic coherent neutron-scattering data. It is thought that the orientational order-disorder phase transition in calcite and the isomorphic phase $NaNO_3$ involves a competing interaction between the actual ordering scheme and alternative ordering schemes that occur with instabilities at different points on the surface of the Brillouin zone of the high-temperature phase (Lynden-Bell et al., 1989; Schmahl and Salje, 1989). Recent single-crystal inelastic coherent neutron-scattering studies of calcite (Dove et al., 1992) have shown the existence of an incipient acoustic phonon instability at the wavevector $\mathbf{k} = [0.5,0,2] \equiv [1.5,0,0]$, described in the hexagonal setting of the low-temperature unit cell. There is a marked anisotropy of the phonon frequencies along different wavevector directions about this point. This application will be described in detail elsewhere (Dove et al., 1992). Another application, which is discussed in this paper, is the calculation of isotope fractionation coefficients for geochemical applications. In the longer term, we plan to use our model for molecular dynamics simulation studies of the orientational order-disorder phase transition in calcite, treating the carbonate group as a rigid body.

In developing our model for calcite, we also included

* Present address: Laboratoire Leon Brillouin, CEN Saclay, 91191 Gif-sur-Yvette, Cedex, France.

0003–004X/92/0304–0244$02.00

aragonite in the fitting procedure with the aim that our model should be fully transferable. As we discuss below, because the data set we used was biased toward calcite the model does not work as well for aragonite.

The model

The microscopic modeling of silicate structures by electrostatic (Coulomb) interactions and short-range few-body potentials has generally been very successful (Catlow, 1988; Price and Parker, 1988; Dove, 1989; Winkler and Buehrer, 1990; Winkler et al., 1991). Our model for $CaCO_3$ follows the same general philosophy.

The Coulomb interaction is evaluated using the Ewald sum. We use a short-range Born-Mayer repulsive potential of the form

$$V(r) = A \exp(-r/\rho) \quad (1)$$

for Ca · · · O and O · · · O interactions, which physically represents the electronic overlap associated with close contact distances between these ion pairs. A similar term was used for the modeling of the internal C · · · O force constant, as will be discussed below. The major differences in the calcite model with respect to the models used for aluminosilicates are associated with modeling the "molecular" CO_3^{2-} group. A purely ionic approach to the description of the CO_3^{2-} group is bound to fail as the directions of the C-O bond are determined by the spatial arrangements of the covalent C-O bonds and are not only due to the minimization of the electrostatic repulsion between the O ions. A pseudocovalent term has been shown to be very important in the modeling of SiO_4 tetrahedra by several workers (Price and Parker, 1988; Catlow, 1988; Dove, 1989; Winkler et al., 1991). This pseudocovalent term takes the form of a bond-bending contribution to the lattice energy and hence is called three-body or bond-bending potential. It is of the form

$$V(\theta) = \tfrac{1}{2}K_{bb}(\theta - \theta_0)^2. \quad (2)$$

We have used this term for the in-plane distortion of the CO_3^{2-} molecular ion, where θ is the instantaneous O-C-O bond angle and θ_0 is taken as 120° in order to represent the isolated molecular ion. The bond-bending term provides only a weak anharmonic force against the movement of the central C atom out of the plane of a molecular ion and no harmonic component. We therefore used an additional four-body, or torsional, term to model the planarity of the CO_3 molecular ion. This torsional term is of the form

$$V(\varphi) = K_t[1 - \cos(2\varphi)] \quad (3)$$

where φ is the angle between two O-C-O planes in a single molecular ion. As we have stated above, without this interaction there is no harmonic restoring force against the out-of-plane movement of the C atom, and the anharmonic restoring forces would not contribute to the calculated harmonic frequencies. The only constraint would come from interactions with the Ca ions and other carbonate groups.

The initial parameters for the O · · · O interactions were taken from the work of Cox et al. (1981) on the modeling of crystals composed of organic molecules (A = 2384.48 eV). The initial parameters for the Ca · · · O interactions were taken from the MEG calculations of Post and Burnham (1986) (A = 6958.304 eV). In the initial stage of the model development, values of the parameters for the short-range Ca · · · O and O · · · O interactions and for the C and O charges were improved by fitting the model against the structures of calcite and aragonite simultaneously, treating the CO_3 group as a rigid molecular ion. Aragonite was included to increase the number of constraints during fitting, and it is reasonable to assume that potential parameters from a good model for calcite should be transferable to aragonite. The values for ρ in each case and the formal Ca charge (+2.0) were not varied. The parameter values for the short-range C · · · O Born-Mayer interaction were then obtained by a trial-and-error method, first by obtaining the gradient of this potential by fitting against the observed C-O bond length (taken as 1.284 Å; Reeder, 1983) and secondly by obtaining the second derivative of the potential by fitting against the frequency of the symmetric stretching vibration (ν_1) of the CO_3 group. For this stage of the work we used the program WMIN (Busing, 1981). As a subsequent stage, the value of the parameter K_t in the torsional interaction (Eq. 3) was chosen so that the calculated value of the torsional vibration of the carbonate ion (ν_2, the mode in which the central C atom moves out of the carbonate plane) was close to the experimental value. The value of the parameter in the O-C-O bond-bending interaction K_{bb} (Eq. 2) was then optimized by fitting against the remaining two internal modes of the CO_3 group (ν_3 and ν_4) that involve the bending of the bonds and asymmetric stretching motions.

For the final refinement of the potential parameters we used the program THBFIT. We fitted the model against the structures and elastic constants of aragonite and calcite simultaneously and also included the internal vibrational frequencies of the CO_3 group in each structure. In total, our model has 11 adjustable parameters that were fitted against 38 observables such as the lattice constants, elastic constants, and phonon frequencies at the Γ point. The values of A and ρ for the Ca · · · O and O · · · O potentials were strongly correlated and could not be optimized simultaneously. Instead we used an iterative procedure to improve the values of these parameters. We did not encounter the same problems with the C · · · O intramolecular potentials. The agreement of the calculated frequencies of the internal modes with experimental data is reasonably good, although it is not possible to get exact agreement for all internal modes since our model does not have enough adjustable parameters. We have chosen to improve the agreement with the bond-bending modes at the expense of the stretching mode. Subsequent trial calculations fitting against the lattice modes of calcite at the Z point—(0,0,½) in the hexagonal setting of the low-temperature unit cell—did not improve the model.

TABLE 1. Potential parameters for the calcite model

	A (eV)	ρ (Å)
Ca · · · O	3943.5977	0.251570
O · · · O	2879.1262	0.252525
C · · · O	1.7411309×10^{13}	0.03873
Ca charge = +1.64203 e		
O charge = −0.894293 e		
C charge = +1.04085 e		
K_{bb} = 3.69441 eV		
K_t = 0.125125 eV		

We also attempted to include an O · · · O dispersive interaction, but we found this did not improve the model and was therefore not included in our final model.

We should stress that the C · · · O interaction we have used should be viewed only as an effective potential that has been designed to give reasonable values for the first and second differential. This interaction can be written as

$$V(r) = \tfrac{1}{2}\alpha(r - r_0)^2 \quad (4)$$

where α = 488.848 eV Å^{-2} and r_0 = 1.3207 Å. The value of r_0 is of course different from the C-O bond length as this potential is merely added to the existing Coulomb interaction and does not exclude the effects of the nearest-neighbor O · · · O interactions. Because of these effects, any other effective potential (such as a Morse potential) will have no more physical meaning than our effective Born-Mayer model. The rather extreme values for A and ρ for the C · · · O interaction follow from the fact that the C-O bond length is rather shorter than found in many other systems, reflecting the essentially covalent aspect of the bonding.

The final set of potential parameters given in Table 1 was used to obtain a relaxed structure of calcite and aragonite at constant pressure, using the program THBREL. The relaxation of the lattice involves the minimization of the static lattice energy by relaxing the atom coordinates, so that there is no residual force acting on any atom and there are no residual bulk strains. Neither the cell parameters nor the symmetry are constrained during the relaxation as all atomic coordinates are varied independently. Harmonic lattice dynamics calculations for calcite were performed on the relaxed structure using the program THBPHON.

RESULTS

The observed and calculated cell parameters and atomic coordinates of the relaxed calcite and aragonite structures are given in Table 2, where they are compared with experimental data. The largest discrepancy is for the value of the calcite c unit-cell parameter, with 1.5% difference, but this magnitude of error is well within the typical limits of such calculations. The calculated and measured elastic constants for calcite and aragonite are given in Table 3. For calcite, all values show reasonably good agreement with experimental data, including the off-diagonal elements. The agreement for the aragonite data is not as good as for calcite, particularly for the small off-diagonal components, but we still regard the comparison as satisfactory. In general, our model tends to give values that are slightly smaller than the experimentally determined values. It should be noted that the discrepancies are all larger than normally might be expected as a result of the neglect of thermal expansion.

TABLE 2. Observed and calculated lattice parameters and atomic coordinates of calcite and aragonite

Lattice constants

		Obs. (Å)	Calc. (Å)	% difference
Calcite $R\bar{3}c$*	a	4.9894	4.9822	0.1
	c	17.039	17.326	1.5
Calcite $R\bar{3}m$** †	a	4.9746	4.9401	0.7
	c	17.619	17.857	1.3
Aragonite $Pmcn$‡	a	4.9598	5.0314	1.0
	b	7.9641	8.0383	0.9
	c	5.7379	5.7394	0.1

Calculated lattice energy (eV)

Calcite $R\bar{3}c$	Calcite $R\bar{3}m$	Aragonite $Pmcn$
−34.38	−34.31	−34.25

Atomic fractional coordinates

		Obs.	Calc.
		Calcite $R\bar{3}c$‖	
O	x	0.2568	0.2578
		Aragonite $Pmcn$§	
Ca	x	¼	¼
	y	0.4150(1)	0.4136
	z	0.7597(3)	0.7603
C	x	¼	¼
	y	0.7622(4)	0.7614
	z	−0.086(1)	−0.073
O1	x	¼	¼
	y	0.9225(4)	0.9203
	z	−0.0962(9)	−0.0764
O2	x	0.4736(4)	0.4700
	y	0.6810(3)	0.6816
	z	−0.0862(5)	−0.0737

* Experimental data are from Dove and Powell (1989) for 300 K.
** Experimental data are from Dove and Powell (1989) for 1165.5 K; the extrapolated value at 1260 K is 17.823 Å.
† Calculated lattice parameters are for a hypothetical (Γ) phase that has all CO_3 groups in the same orientation, as described in the text.
‡ Experimental data are from Dickens and Bowen (1971) for 300 K.
‖ Experimental data from Reeder (1983). Note that all other coordinates are fixed by symmetry.
§ Experimental data from De Villiers (1971) for 300 K. Estimated errors on the last significant figures are given in brackets.

The vibrational frequencies at $\mathbf{k} = 0$ have been thoroughly studied for calcite, and a review of infrared and Raman data has been given by Farmer (1974). Phonon dispersion curves have been measured by Cowley and Pant (1973) and Dove et al. (1992). Tables 4 and 5 show a comparison of calculated and measured phonon frequencies. At the Z point the agreement is very good: the largest deviation is less than 10% of the observed frequencies. At the Γ point the agreement is mostly good, but for the very low-frequency modes and for the high-frequency external modes only satisfactorily. In part these discrepancies arise from the failure to calculate the mode anticrossings at exactly the correct wavevector. It should be noted that the highest frequency pair of external branches has not been measured, and these are not shown in Figure 1.

Table 3. Comparison of calculated elastic constants (in Mbar) of calcite and aragonite with observed data

	Calcite		
	Observed*	Calculated	Calculated Γ phase
C_{11}	1.463	1.295	1.221
C_{33}	0.853	0.734	0.863
C_{44}	0.340	0.279	0.241
C_{12}	0.597	0.478	0.478
C_{13}	0.508	0.441	0.411
C_{14}	−0.208	−0.135	−0.127
	Aragonite		
	Observed**	Calculated	
C_{11}	1.60	1.46	
C_{22}	0.87	0.85	
C_{33}	0.85	0.70	
C_{44}	0.41	0.33	
C_{55}	0.26	0.22	
C_{66}	0.43	0.34	
C_{12}	0.37	0.48	
C_{13}	0.02	0.23	
C_{23}	0.16	0.35	

* Experimental data from Dandekar (1968).
** Experimental data from Hearmon (1946).

Figure 1 shows a comparison of the calculated dispersion curves for wavevectors along the three-fold axis with the experimental data of Cowley and Pant (1973). Figure 2 shows a comparison of the calculated and measured acoustic phonon dispersion curves along [1,0,4]. Our model clearly reproduces the softening of the transverse acoustic mode. This mode is important for the behavior of the order-disorder phase transition observed at 1260 K (Dove and Powell, 1989; Dove et al., 1992). The actual kinks in the longitudinal mode dispersion curve arise from many anticrossing interactions with other modes, which are indicated by our calculations but which are not shown in the figure for clarity, and it is quite possible that these anticrossings are hidden in the experimental data. A more detailed discussion of the dispersion curves along this direction will be presented in our report on our recent inelastic coherent neutron-scattering studies of calcite (Dove et al., 1992), where we also use the present model to provide quantitative information on the energetics of spontaneous structure fluctuations.

Table 4. Comparison of the calculated and observed frequencies (in THz) of the external modes of calcite

Γ point			Z point		
Mode	Obs.*	Calc.	Mode	Obs.*	Calc.
Γ_3'	2.9	3.9	$Z_{2/3}$	2.9	2.6
Γ_1'	4.0	5.7	Z_1	4.3	4.2
Γ_3	4.7	4.1	$Z_{2/3}$	5.3	5.2
Γ_2	5.2	5.8	Z_1	5.6	6.1
Γ_3'	6.6	6.6	$Z_{2/3}$	8.8	8.3
Γ_3	8.4	8.5	Z_1	—	10.4
Γ_3'	9.1	8.5			
Γ_2'	9.3	8.1			
Γ_1	—	8.5			
Γ_2	—	11.3			

* Experimental data from Cowley and Pant (1973).

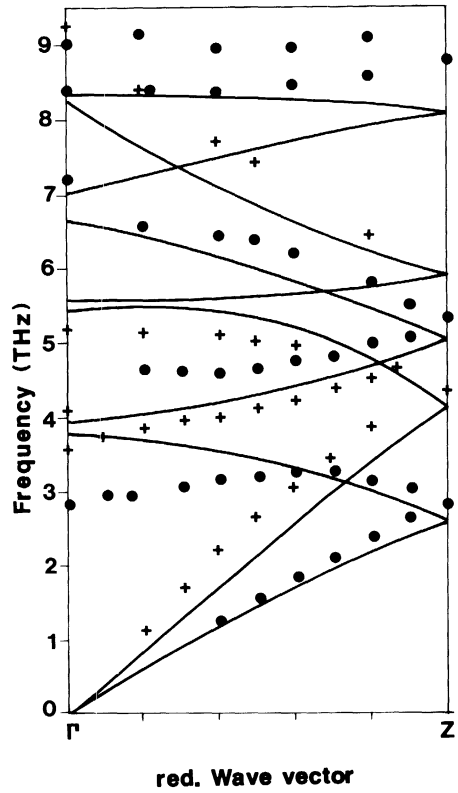

Fig. 1. Comparison of experimentally determined (Cowley and Pant, 1973) and calculated phonon dispersion curves in calcite along the triad axis. Γ denotes the wavevector at the center of the Brillouin zone, and Z denotes the Brillouin zone boundary wavevector [0,0,1.5]. The filled circles represent double-degenerate modes, and the crosses represent single modes.

The results for calcite are better than for aragonite. In particular we note that the model predicts that aragonite is unstable against a displacive phase transition at the wavevector **c***/2. This shows itself as an imaginary calculated frequency of a degenerate mode at this wavevector, which causes the two branches at other wavevectors in the vicinity of **c***/2 also to be imaginary. Given that we have noted that the phonon frequencies in calcite are fairly sensitive to the details of the potential model, we believe that this deficiency might have been avoided if we had been able to include phonon frequencies for aragonite in the fitting database. It should be noted that the

Table 5. Internal modes of calcite (in THz) averaged over the Davydov splitting

	Mode	Observed*	Calculated
C-O symmetric stretching mode	ν_1	32.6	30.7
Torsional mode	ν_2	26.4	26.9
Bond bending modes	ν_3	43.9	42.6
	ν_4	21.4	21.0

* Experimental data from Farmer (1974).

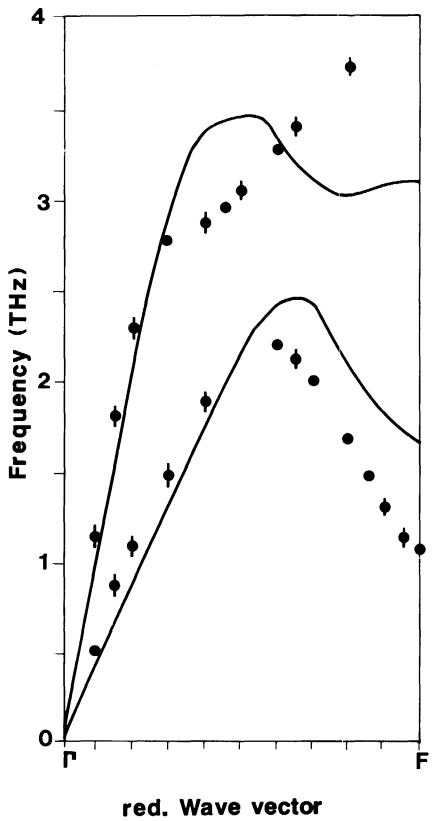

Fig. 2. Observed (Dove et al., 1992) and calculated softening of a transverse acoustic phonon in calcite along [1,0,4]. Γ denotes the wavevector at the center of the Brillouin zone, and F denotes the Brillouin zone boundary wavevector [0.5,0,2].

reasonable agreement with the elastic constants arises from the fact that the symmetries of the unstable modes are not the same as the relevant acoustic modes, so that there is no interaction between these modes. It would be interesting to investigate the possible existence of an anomalous low-frequency mode at the wavevector **c***/2 in aragonite by inelastic coherent neutron scattering. Accordingly we cannot take the relative lattice energies of calcite and aragonite given in Table 2 too seriously.

Applications

Fractionation coefficients

One application for lattice dynamics calculations is the determination of isotope fractionation coefficients. A summary of the thermodynamics of isotopic fractionation has been given by Kieffer (1982). Following Kieffer (1982) we quote the result:

$$\ln f = \frac{F^* - F}{-k_B T} + \frac{3r}{2} \ln \frac{m}{m^*} \qquad (5)$$

where F is the Helmholtz free energy, f is the reduced fractionation factor, r is the number of atoms of the element being exchanged, m is the respective mass, and

Table 6. Reduced isotope fractionation coefficient (r^{-1} 1000 ln f) for $^{16}O/^{18}O$ calcite and reduced isotope fractionation factor (10^3 ln $\alpha_{calcite\text{-}H_2O}$) for calcite-$H_2O$ fractionation

Temperature (K)	Kieffer (1982)	Experiment	This study
		$r^{-1}10^3$ ln f ($^{16}O/^{18}O$)	
298	98.93*		94.81
500	41.43*		39.35
773	18.38*		17.67
1000	11.38*		10.82
		10^3 ln $\alpha_{calcite\text{-}H_2O}$	
298	28.1** †	28‡	24†
773	0.27** ‖	1.19§, 1.76‡	−0.44‖
998	−0.981** ‖	−0.10‡	−1.541‖
1000	−0.2** †	−0.2‡	−0.7†

* Values from Kieffer model as given by Clayton et al. (1989).
** Values from Kieffer (1982).
† Using the values for the reduced partition function of H_2O as cited by Kieffer (1982) from Becker (1971): 1000 ln f at 298 K = 70.81; 1000 ln f at 1000 K = 11.55
‡ Data from Friedman and O'Neil (1977), extrapolated for $T > 773$ K.
‖ Using the values for the reduced partition function of H_2O from Bottinga and Javoy (1973): 1000 ln f at 773 K = 18.110; 1000 ln f at 998 K = 12.361.
§ Clayton et al. (1989), error is 0.12.

starred symbols refer to the heavy isotope. The Helmholtz free energy for any substance can be calculated from its phonon density of states (Born and Huang, 1954). For this we used a regular spaced grid with 1000 points throughout the whole of the Brillouin zones of ^{16}O calcite and ^{18}O calcite. Our calculated values for f are compared with the data of Kieffer (1982) in Table 6 (additional data of Kieffer not given in Kieffer, 1982, are cited in Clayton et al., 1989). No experimental data for the reduced partition function of calcite are available. Our calculated values are consistently 5% smaller than the values of Kieffer (1982). This is principally because Kieffer used modified frequency values in order to improve the agreement with the fractionation coefficients for calcite-H_2O (see below).

Experiments provide fractionation factors for isotope exchanges between different phases. Experimental data for the O isotope exchange between calcite and H_2O are given in Table 6. Fractionation coefficients for H_2O have been calculated by Becker (1971) as cited by Kieffer (1982) and by Bottinga and Javoy (1973). Using these values for H_2O and values given by our model for calcite, we get a moderate agreement between experiment and calculated values (Table 6). The reason for the discrepancies is not clear. A discussion of possible errors in these calculations has been given by Clayton et al. (1989), who note the possibilities of systematic errors in hydrothermal experiments, in the calculated partition functions of the solids, and in the calculated partition function of H_2O.

High-temperature studies

Calcite undergoes an orientational order-disorder phase transition at 1260 K (Dove and Powell, 1989). The carbonate groups in the high-temperature phase ($R\bar{3}m$, Z = 1) are disordered with respect to 60° rotations about the threefold axes, whereas in the low-temperature phase the

carbonate groups in a single (0001) plane (indexed on the basis of a hexagonal cell) have identical orientations, but the groups in neighboring planes are rotated by 60° (called Z ordering because the ordering instability occurs at the Z point on the surface of the Brillouin zone of the high-temperature phase). The data of Dove and Powell (1989) show that, on heating, lattice parameter a decreases from 4.9894 Å at 300 K to 4.9746 Å at 1165.6 K, whereas lattice parameter c increases in the same temperature interval from 17.039 Å to 17.619 Å.

The application of static lattice energy minimization and lattice dynamics calculations to phase transitions where the high-temperature phase is stabilized by dynamic effects, such as the jump diffusion of a molecular group, is of course limited. Nevertheless, neglecting stabilizing dynamical effects and considering average macroscopic effects only, we hoped to calculate the influence of the short-range correlations by treating, in a zeroth order approximation, the high-temperature phase as a superposition of the low-temperature phase and a phase in which the carbonate groups all have the same orientation (called the Γ phase, with space group $R\bar{3}m$, $Z = 1$). We calculated the lattice and elastic constants for this hypothetical Γ phase, and the results are given in Tables 2 and 3. The model for the hypothetical Γ phase gives a very large increase of lattice parameter c and a decrease in lattice parameter a. In our zeroth order approximation we can equate the cell parameters of the high temperature with the averages over the cell parameters for the Z and Γ phases. Accordingly we predict the large spontaneous strain that gives rise to the thermal expansion of the c lattice constant and the anomalous shrinkage of the a lattice constant. We can therefore deduce that a large part of the spontaneous strain that accompanies the transition is due to the occurrence of short range order in which carbonate groups of different layers have the same orientation. The calculation of the elastic constants for the Γ phase shows that the C_{33} elastic constant increases significantly (by 15%), whereas C_{11} and C_{44} decrease (by 6% and 14%, respectively). These changes are due to the increased O-O repulsion between different CO_3 groups.

Conclusion

We believe that the interatomic potential model for calcite presented in this paper is a substantial improvement on previous models (e.g., Singh et al., 1987). It is versatile and gives better unit-cell parameters, elastic constants, and phonon frequencies than before. It has been applied in a geochemical context, and it has been shown that it may be used in the interpretation of new inelastic coherent neutron-scattering data. The use of the potential parameters in molecular dynamics simulation calculations (assuming a rigid CO_3 group) should be straightforward, and these calculations are planned for the near future. The rigid ion model described here will be adequate for most applications. We think that any further improvement will require inclusion of a shell model for the description of the O ions. It is also clear that better results for aragonite could be obtained if we were able to include the phonon frequencies for aragonite in the fitting database. However, because of the relative complexity of the aragonite structure, this is not trivial.

Acknowledgments

We would like to acknowledge helpful discussions with G.D. Price (University College London) and R. Jackson (University of Keele). We are grateful for time on the computers of the Bullard Laboratories and the Institute of Theoretical Geophysics, University of Cambridge, and the support of the system manager, D. Lyness. E.K.H.S. is indebted to the Leverhulme Foundation for financial support; B.W. is grateful for a grant from the DAAD (German Academic Science Foundation); M.J.H. is grateful for financial support from NERC (U.K.); and M.T.D. is grateful to a grant from the Royal Society (U.K.) for provision of computing facilities. The suite of programs used in this study, THBFIT, THBREL, and THBPHON, are supported by CCP5 SERC, Daresbury Laboratory, Warrington, Cheshire WA4 4AD, U.K.

References cited

Becker, R.H. (1971) Carbon and oxygen isotope ratios in iron formation and associated rocks from the Hamersley Range of Western Australia and their implications. Ph.D. thesis, Department of Chemistry, University of Chicago, Chicago.

Born, M., and Huang, K. (1954) Dynamical theory of crystal lattices. Oxford University Press, Oxford, U.K.

Bottinga, Y., and Javoy, M. (1973) Comments on oxygen isotope geothermometry. Earth and Planetary Science Letters, 20, 250–265.

Busing, W.R. (1981) WMIN, a computer program to model molecules and crystals in terms of potential energy functions. Oak Ridge National Laboratory Report ORNL 5747.

Catlow, C.R.A. (1988) Computer modelling of silicates. In E.K.H. Salje, Ed., Physical properties and thermodynamic behaviour of minerals, p. 619–638. Riedel, Dortrecht, Holland.

Clayton, R.N., Goldsmith, J.R., and Mayeda, T.K. (1989) Oxygen isotope fractionation in quartz, albite, anorthite and calcite. Geochimica et Cosmochimica Acta, 53, 725–733.

Cowley, R.E., and Pant, A.K., (1973) Lattice dynamics of calcite. Physical Review, B8, 4795–4800.

Cox, S.R., Hsu, L.-Y., and Williams, D.E. (1981) Nonbonded potential function models for crystalline oxyhydrocarbons. Acta Crystallographica, A37, 293–301.

Dandekar, D.P. (1968) Elastic constants of calcite. Journal of Applied Physics, 39, 2971–2973.

De Villiers, J.P.R. (1971) Crystal structures of aragonite, strontianite and witherite. American Mineralogist, 56, 758–767.

Dickens, B., and Bowen, J.S. (1971) Refinement of the crystal structure of the aragonite phase of $CaCO_3$. Journal of Research of the National Institute of Standards. Physics and Chemistry, 75A, 27–32.

Dove, M.T. (1989) On the computer modelling of diopside: Toward a transferable potential for silicate minerals. American Mineralogist, 74, 774–779.

Dove, M.T., and Powell, B.M. (1989) Neutron diffraction study of the tricritical orientational order/disorder phase transition in calcite at 1260 K. Physics and Chemistry of Minerals, 16, 503–507.

Dove, M.T., Hagen, M., Harris, M.J., Powell, B.M., Steigenberger, U., and Winkler, B. (1992) Anomalous inelastic neutron scattering from calcite. Journal of Physics: Condensed Matter, in press.

Farmer, V.C. (1974) Infrared spectroscopy of minerals. Mineralogical Society, London.

Friedman, I., and O'Neil, J.R. (1977) Compilation of stable isotope fractionation factors of geochemical interest. Geological Survey Professional Paper 440—KK, United States Government Printing Office, Washington, DC.

Hearmon, R.F.S. (1946) The elastic constants of anisotropic materials. Reviews of Modern Physics, 18, 409–440.

Kieffer, S.W. (1982) Thermodynamics and lattice vibrations of minerals: 5. Applications to phase equilibria, isotopic fractionation and high-

pressure thermodynamic properties. Reviews of Geophysics and Space Physics, 20, 827–849.

Lynden-Bell, R.M., Ferrario, M., McDonald, I.R., and Salje, E. (1989) A molecular dynamics study of orientational disordering in crystalline sodium nitrate. Journal of Physics: Condensed Matter, 1, 6523–6542.

Post, J.E., and Burnham, C.W. (1986) Ionic modelling of mineral structures and energies in the electron gas approximation: TiO_2 polymorphs, quartz, forsterite, diopside. American Mineralogist, 71, 142–150.

Price, G.D., and Parker, S.C. (1988) The computer simulation of the lattice dynamics of silicates. In E.K.H. Salje, Ed., Physical properties and thermodynamic behaviour of minerals, p. 591–618. Riedel, Dortrecht, Holland.

Reeder, J.R. (1983) Crystal chemistry of the rhombohedral carbonates. In Mineralogical Society of America Reviews in Mineralogy, 11, 1–48.

Schmahl, W.W., and Salje, E. (1989) X-ray diffraction study of the orientational order/disorder transition in $NaNO_3$: Evidence for order parameter coupling. Physics and Chemistry of Minerals, 16, 790–798.

Singh, R.K., Gaur, N.K., and Chaplot, S.L. (1987) Lattice dynamics of molecular calcite crystals. Physical Review, B35, 4462–4471.

Winkler, B., and Buehrer, W. (1990) Lattice dynamics of andalusite: Prediction and experiment. Physics and Chemistry of Minerals, 17, 453–461.

Winkler, B., Dove, M.T., and Leslie, M. (1991) Static lattice energy minimization and lattice dynamics calculation of aluminosilicate minerals. American Mineralogist, 76, 313–331.

Manuscript received November 2, 1990
Manuscript accepted October 9, 1991